Editors' Suggestion

Surface Resonant Raman Scattering from Cu(110)

M. Denk,[1,2,*] E. Speiser,[1] J. Plaickner,[3,1] S. Chandola,[3,1] S. Sanna,[4] P. Zeppenfeld,[2] and N. Esser[5,1]

[1]*Leibniz-Institut für Analytische Wissenschaften—ISAS—e.V., Schwarzschildstrasse 8, 12489 Berlin, Germany*

[2]*Institute of Experimental Physics, Johannes Kepler University, Linz, Altenberger Strasse 69, 4040 Linz, Austria*

[3]*Helmholtz-Zentrum Berlin für Materialien und Energie GmbH, Hahn-Meitner-Platz 1, 14109 Berlin, Germany*

[4]*Institut für Theoretische Physik and Center for Materials Research (LaMa), Justus-Liebig-Universität Gießen, Heinrich-Buff-Ring 16, 35392 Gießen, Germany*

[5]*Institut für Festkörperphysik, Technische Universität Berlin, Hardenbergstrasse 36, 10623 Berlin, Germany*

(Received 2 May 2021; revised 17 November 2021; accepted 3 April 2022; published 26 May 2022)

We report the first evidence of Raman scattering from surface phonons of a pristine metal surface. Our study reveals a Raman-active surface vibrational resonance on Cu(110) with a surprisingly large scattering efficiency. With the incident photon energy close to the energy of the Cu(110) surface state electronic transition, the Raman scattering from the surface optical resonance can be significantly enhanced, while any contribution from bulk phonons is absent.

DOI: 10.1103/PhysRevLett.128.216101

Raman spectroscopy is a standard technique for studying the lattice dynamic properties of solids [1,2], including surfaces and interfaces [3]. Advances in the field of surface-enhanced Raman spectroscopy (SERS) and tip-enhanced Raman spectroscopy (TERS) have facilitated access to nanoscale structures in this regard [4,5].

Moreover, since the first evidence of Raman lines from surface vibrational modes on Sb-terminated InP(110), further studies have suggested that surface-related Raman scattering is a general property of solid surfaces [3,6,7]. In this context, resonant Raman spectroscopy (RRS) is often used to selectively enhance the surface Raman signal to compensate for the limited scattering volume of the surface compared to the bulk. In RRS, the excitation energy is chosen close to an electronic transition of the material, i.e., at interband critical points. If surface electronic transitions are involved, the Raman intensity of a surface vibrational mode can thus be significantly increased [2,3]. Despite the success of Raman spectroscopy in the study of surface phonons, most research to date has been on semiconducting materials [3,8,9]. Bulk metals have only been the subject of a limited number of Raman scattering experiments [10–12], since optical phonon modes require the presence of a non-primitive lattice unit cell. In addition, screening significantly reduces the scattering efficiency because in bulk metals the lifetime of electron-hole pairs is too short to interact effectively with the crystal lattice via the Raman effect [13,14]. At metal surfaces, however, a less efficient screening can significantly increase the lifetime of electron-hole pairs [15,16], particularly if electronic transitions related to surface states are involved in the Raman process [17].

In the bulk of solids with a single atom per unit cell, such as cubic metals (i.e., sc, bcc, or fcc), solely acoustic phonons exist, which can only be excited in scattering processes of higher order. In first-order inelastic scattering from acoustic modes, the frequency shifts are usually too small to be observed in Raman experiments. However, for silver and gold nanocrystals, it was possible to obtain a Raman signal mapping the bulk phonon density of states [18,19], with the challenging measurement of acoustic phonons enabled by Raman scattering in resonance with plasmonic transitions. First-order Raman scattering from *surface optical phonons*, on the other hand, should be possible even for metals with only one atom in the bulk unit cell. Such optical surface modes arise from the reduced symmetry at the surface: Since the translational symmetry along the surface normal is lifted, the relevant unit cell extends over the entire semi-infinite crystal and contains more than just one atom. As a consequence, surface modes with $\omega > 0$ exist at the center of the surface Brillouin zone. The present study shows that Raman scattering from these surface phonon modes can indeed be observed for Cu(110), opening new possibilities for the use of Raman spectroscopy to study surface resonances in metals. Given the recent developments in the field of TERS [20,21], a comprehensive understanding of the underlying physical effects will be of great significance.

Figure 1 shows Raman spectra for Cu(110) recorded at room temperature in ultrahigh vacuum using discrete laser lines for excitation. Experimental details are given in the Supplemental Material [22]. A sharp peak at a Raman shift of 161.5 cm^{-1} (20 meV) can be seen in Fig. 1, particularly

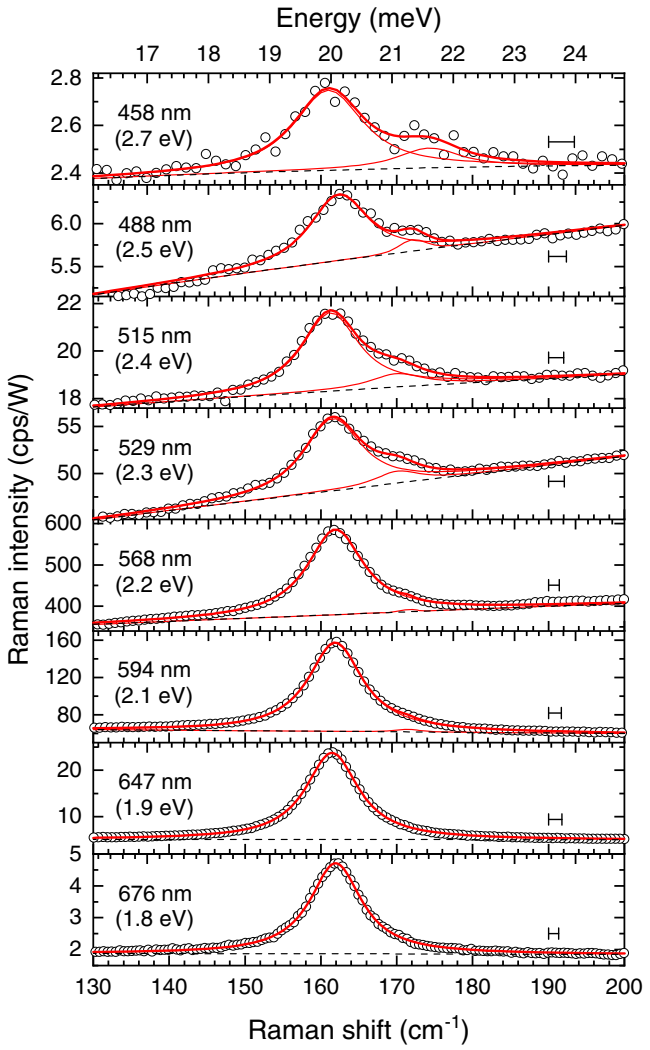

FIG. 1. Raman spectra for Cu(110) (open circles). Wavelength and energy of the incident laser light are given on the left side of each spectrum. The spectral features were fitted to Voigt curves on a 5th order polynomial background. The background, Voigt components, and the sum curve are shown separately. The spectral resolution determined from the width of the plasma lines used for energy calibration is given on the right. The resolution was used as a constant Gaussian component in the Voigt fitting procedure.

for the spectra with incident laser energies between 2 and 2.4 eV. A Raman shift of 161.5 cm^{-1} agrees well with the excitation energy of the Cu(110) surface phonon resonance, as observed in previous EELS and HAS studies [36,37]. This surface phonon resonance is mainly confined to the topmost few surface layers, with the entire layer of surface atoms moving in the direction normal to the surface, out of phase with the second layer atoms and in-phase with the atoms in the third layer, etc. [36,38], as shown in Fig. 2(c).

The Raman scattering signal at 161.5 cm^{-1} is strongly dependent on the energy of the incident laser, peaking at 2.2 eV, with significant intensity observed only within a narrow energy range of 0.5 eV. This dependence on excitation energy is a clear indication of resonant enhancement of Raman scattering in the vicinity of optical transitions involving surface electronic states. Indeed, angle-resolved photoemission and inverse photoemission studies have found an occupied surface state 0.4 eV below the Fermi level E_F at the $\bar{Y}$ point of the Cu(110) surface Brillouin zone (SBZ), and an unoccupied state 1.8 eV above E_F [39,40]. Both electronic surface states are confined to the topmost atomic layer and rapidly decay within a few lattice planes towards the bulk [41]. Transitions between these surface states were observed by reflection anisotropy spectroscopy at an energy of 2.1 eV [42–44], close to the laser excitation energy at which the largest enhancement of Raman scattering is seen in Fig. 1.

The Cu(110) surface phonon resonance involves a large relative displacement of the first and second layer atoms of the surface. The surface electronic states and, consequently, the optical transition energy will be strongly affected by a modulation of the respective interlayer spacing Δz. In fact, the energy of the optical transition decreases linearly upon a temperature-induced (static) increase of Δz [44]. A significant variation of the electronic energy levels due to excitation of the phonon mode will result in a large deformation potential $dE/d\Delta z$ and, hence, a large Raman cross section [1,2]. To verify whether coupling of the surface phonon resonance and this particular transition indeed increases the Raman scattering at 161.5 cm^{-1} in Fig. 1, model calculations in the framework of density functional theory (DFT) were performed for the surface electronic structure of Cu (110), and for the normal mode frequencies and displacement patterns (see Ref. [22] for details). The electronic band structure calculated along high-symmetry directions in the surface Brillouin zone is shown together with the projected bulk bands in Fig. 2(a). The band structure in Fig. 2(a) is consistent with previous DFT calculations [41]: The specific, surface-localized optical transition occurs in the vicinity of the $\bar{Y}$ point with a transition energy E between 2.1 and 2.2 eV, from the partially occupied to the unoccupied surface states indicated by b_1 and b_2 in Fig. 2(a), respectively.

In a subsequent lattice dynamics calculation a z-polarized surface mode according to the surface phonon resonance was identified at 173 cm^{-1}. To simulate the influence of this vibration on the electronic states, the band structure was calculated for different static values of the interlayer distance of the topmost two lattice planes. The calculation yields a strong response of the electronic surface states to a movement of these atomic layers. In particular, Fig. 2(b) shows the variation of the spacing between Cu layer one and two (Δz) and the resulting variation of the distance between b_1 and b_2 (ΔE) during a single period of the vibration. Thus, Raman scattering occurs via the deformation potential. In addition, scattering due to electron density fluctuations at the surface contributes as b_1 shifts with respect to the Fermi level during oscillation. The combination of both mechanisms then leads to the strong enhancement of the Raman

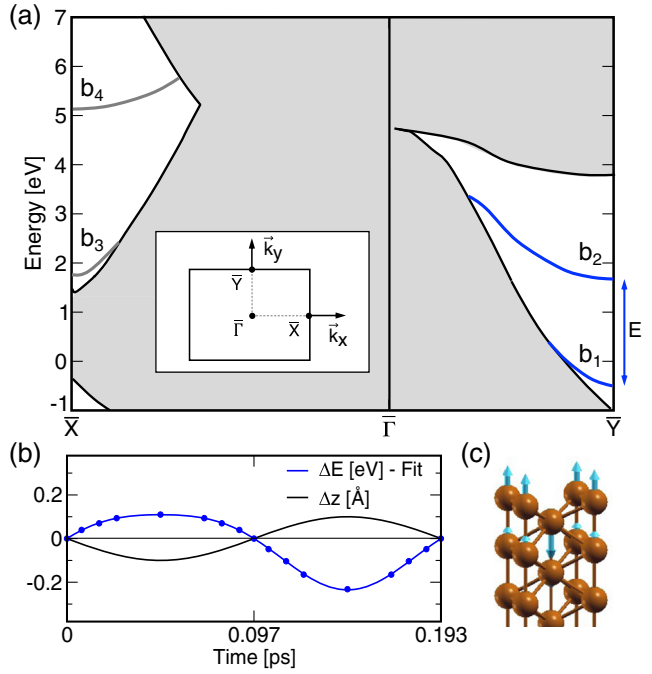

FIG. 2. (a) Calculated electronic band structure of Cu(110): Surface states are labeled b_i, the surface-projected bulk bands are overlaid in gray. The inset shows the SBZ with the symmetry points used for the calculation. (b) Variation of the spacing of the upper two atomic planes of the Cu lattice (Δz) and resulting variation of the distance between b_1 and b_2 at $\bar{Y}$ (ΔE), for a single oscillation period. The fit through the ΔE points serves as a guide to the eyes. (c) Vibrational pattern of the surface phonon resonance.

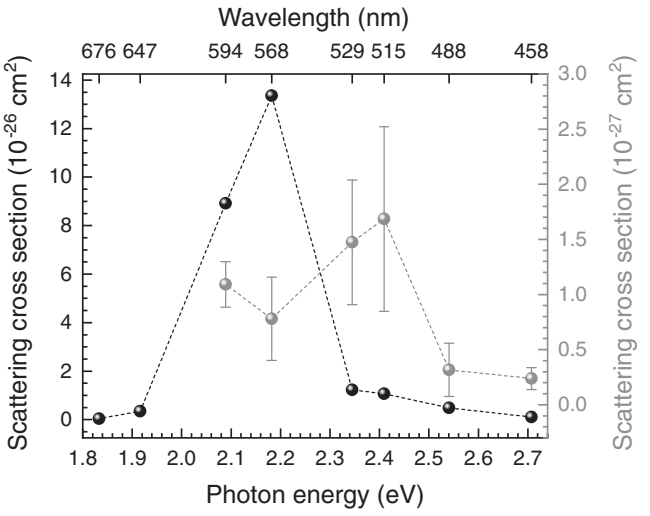

FIG. 3. Absolute scattering cross section of Cu(110), for the surface phonon resonance at 161.5 (black) and the mode at 172 cm^{-1} (gray).

scattering at 161.5 cm^{-1} in Fig. 1. However, the extent to which scattering occurs via deformation potentials or via charge density fluctuations cannot be determined in this way. Yet, the corresponding DFT calculation shows that for in-plane polarized phonons no coupling with the optical transition at the $\bar{Y}$ point can occur, since occupation of adjacent modes with displacement along x or y does not affect the surface states b_1 and b_2.

In the spectra in Fig. 1, a weak feature at a Raman shift of 172 cm^{-1} (21.3 meV) can be seen. Again the intensity is resonantly enhanced, similar as for the Raman peak at 161.5 cm^{-1}. The maximum energy of this second enhancement, although it is slightly higher than for the peak at 161.5 cm^{-1}, cannot be precisely determined due to the vicinity of the strong main resonance. However, optical contributions at energies slightly higher than the surface state transition have been reported and are due to transitions involving bulk-related electronic states [44,45].

Figure 3 shows the absolute scattering cross section for the surface phonon resonance at 161.5 cm^{-1} and the second mode at 172 cm^{-1}, respectively, as a function of the optical excitation energy. The cross section was calculated after Ref. [46] as described in Ref. [22]. The scattering length for both modes is $d = 1.278$ Å, i.e., the interlayer distance in bulk Cu. The resulting resonance profile for the mode at 161.5 cm^{-1} shows a sharp peak centered at a photon energy of 2.2 eV. Compared to the energy of the electronic transition of the Cu(110) surface states, the resonance peak is slightly shifted to higher energies (≈0.1 eV). The resonance curve for the second mode has a feature at about 2.3 eV, also slightly higher than the energy of the surface-modified bulk transition. However, the scattering cross section curves in Fig. 3 are in perfect agreement with the optical absorption due to surface state transition and modified bulk transition in Ref. [44], respectively.

To understand in detail the spectral signature of the Raman intensity in Fig. 1, additional lattice dynamics calculations were performed, based on a force-constant model fitted to the experimentally determined dispersion curves of the Cu(110) surface phonons [37]. The phonon dispersion curves thus obtained for the high-symmetry direction $\bar{\Gamma}\bar{Y}$ are shown on the right side in Fig. 4. For a slab containing N layers the calculation yields $3N - 3$ optical modes at the $\bar{\Gamma}$ point with energies up to 29.8 meV, the maximum energy for Cu bulk phonons [37]. The surface phonon resonance lies at around 19.7 meV and arises from a pseudo band gap in the dipole-active phonon density of states for longitudinal phonons propagating perpendicular to the (110) surface [36]. The phonon dispersion in Fig. 4 shows a large number of modes which merge into a van Hove singularity at 21 meV as a result of the projection of the bulk phonon branches at the X point onto the $\bar{\Gamma}$ point of the surface Brillouin zone. The surface splits off a mode from this region of high density of bulk-phonon states into the pseudo-band-gap region where the strong depletion of the projected density of states causes the mode to become a surface resonance. By determining the spectral densities the slab-model calculation provides the polarization and intensity of each eigenmode. The left

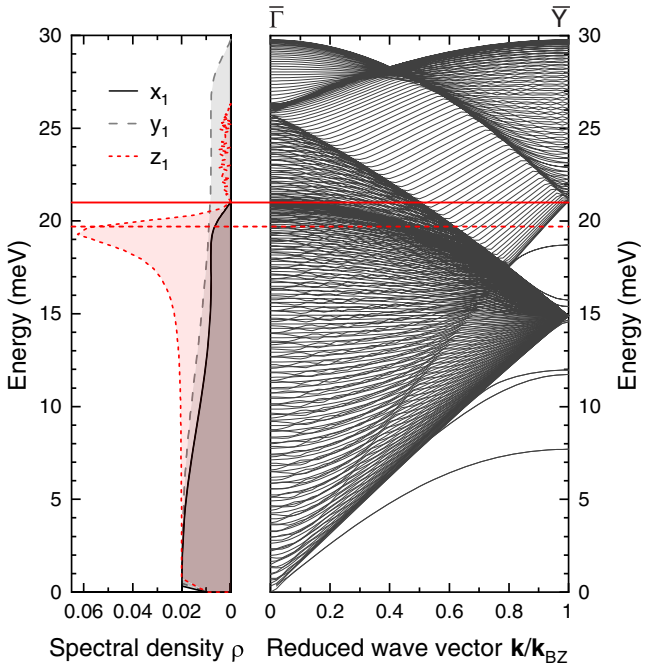

FIG. 4. Phonon dispersion curves for Cu(110) along $\bar{\Gamma}\,\bar{Y}$ (right panel) and spectral density ρ at the $\bar{\Gamma}$ point for displacement of the first layer Cu atoms along the directions x, y, and z (left panel), obtained from the lattice dynamical calculation described in Ref. [22]. The solid line marks the region of high density of surface-projected bulk phonon states at 21 meV, the dashed line the surface phonon resonance at 19.7 meV.

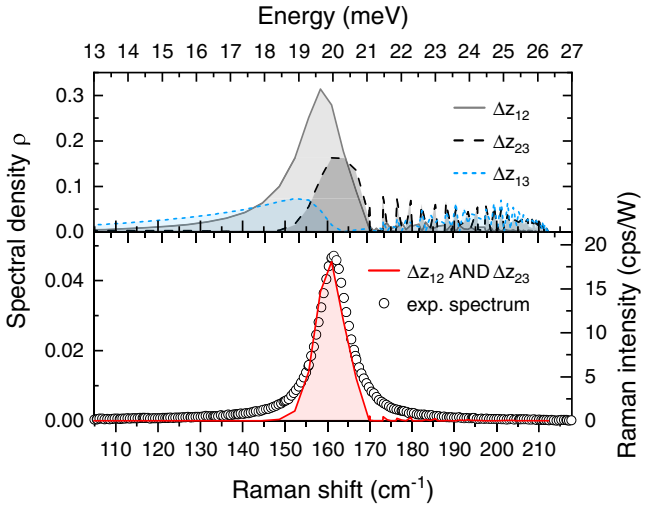

FIG. 5. Spectral densities ρ for relative displacements Δz_{12}, Δz_{23}, and Δz_{13}, respectively (top), and combined ρ for relative displacements Δz_{12} and Δz_{23}, compared to an experimental Raman spectrum obtained at 1.9 eV (bottom). The background was subtracted from the spectrum.

side in Fig. 4 shows the resulting ρ for the first layer atoms and displacement along x, y, and z. As before, only modes with displacement along the surface normal z can possibly contribute to the measured Raman signal in the spectra in Fig. 1. Moreover, it becomes clear that a displacement of the atoms in the first Cu layer (ρ_z) alone cannot account for the sharp Raman peak at 161.5 cm^{-1}.

If we define the relative spectral density $\rho_{\Delta z_{ij}}$ as the z displacement of the atoms of a specific layer i with respect to the atoms of another layer j, the z component of the overall displacement pattern of the surface phonon resonance can be gradually constructed. Relative spectral densities $\rho_{\Delta z_{12}}$ for the atoms in the first and second layer and $\rho_{\Delta z_{23}}$ for those in the second and third layer, respectively, are shown in the upper graph in Fig. 5. Both curves refer to spectral densities for which the interlayer spacing changes during the vibration. The third curve in the graph shows the spectral density $\rho_{\Delta z_{13}}$ for the atoms in layer one and three, which move in phase. The bottom panel of Fig. 5 shows a Raman spectrum for comparison. The qualitative agreement of the spectral densities $\rho_{\Delta z_{12}}$ as well as $\rho_{\Delta z_{23}}$ with the experimental spectrum confirms that the Raman scattering amplitude is indeed correlated with the antiphase displacement of the atomic layers in the surface-near region along z. Nevertheless, to further approximate the experimental line shape, both spectral densities must be considered together. The resulting combined spectral density $\rho_{\Delta z_{13}} \times \rho_{\Delta z_{23}}$, also in the bottom panel of Fig. 5, agrees perfectly with the experimental spectrum. In particular, the combined ρ curve reproduces the narrow width and symmetrical line shape of the peak in the Raman curve.

This indicates that the region of the coupling of surface phonon resonance and electronic surface states extends slightly deeper into the crystal than just the second layer. Thus, it is essential to include all parts of the vibration which have influence on the surface electronic states to reproduce the experimental Raman spectrum. Nevertheless, the measured Raman intensity at 161.5 cm^{-1} arises exclusively from the topmost few layers of the crystal, also because any contribution from higher-order scattering is absent in the spectra. At least a small intensity from scattering by acoustic phonons is expected, since the penetration depth of the incident light is large enough ($\approx$14 nm at 1.9 eV) and resonant enhancement due to excitation in the vicinity of bulk electronic transitions would be possible. However, the intensity at around 172 cm^{-1} (21.3 meV) in Fig. 1 is most likely due to scattering by surface-projected bulk phonons in the surface-near region. This projection of the acoustic bulk phonon branches leads to a large density of states at the $\bar{\Gamma}$ point of the surface Brillouin zone at 21 meV. Because of the slightly higher energy of the optical resonance of the 172 cm^{-1} Raman feature it cannot be related to scattering in resonance with the surface state electronic transition. Most likely, transitions between bulk states modified at the surface are involved. Excitation in resonance with these transitions then leads to enhanced Raman scattering by the surface-projected bulk phonon modes. The comparably low intensity of this "bulk-related" signal further corroborates that a significant enhancement of the Raman intensity in Cu can

only be obtained if the phonons and the electronic transition are *both* strongly localized in the surface-near region.

In conclusion, the present study shows the first evidence of Raman scattering from surface phonons on a metal surface. Our experiments demonstrate the existence of Raman-active surface optical phonons on Cu(110) with large scattering efficiency. In addition to the symmetry reduction at the surface required to ensure optical phonon modes, an optical excitation in resonance with electronic transitions localized in the surface region is crucial for the observation of Raman scattering from metal surfaces.

Financial support by the Ministry for Culture and Science NRW, The Governing Mayor of Berlin–Senate Chancellery Higher Education and Research, and the German Federal Ministry of Education and Research (BMBF) is gratefully acknowledged. S. C. and J. P. would like to thank the BMBF additionally as part of the project CatLab (03EW0015A). M. D. acknowledges financial support from the Austrian Science Fund (FWF): Project No. J 4437-N. S. S. acknowledges the support of the LOEWE Program of Excellence of the Federal State of Hesse (LOEWE Focus Group PriOSS "Principles of On-Surface Synthesis").

*Corresponding author.
mariella.denk@jku.at

[1] *Light Scattering in Solids I*, edited by M. Cardona, Topics Appl. Phys. Vol. 8 (Springer-Verlag, Berlin, Heidelberg, 1975).
[2] *Light Scattering in Solids II*, edited by M. Cardona and G. Güntherodt, Topics Appl. Phys. Vol. 50 (Springer-Verlag, Berlin, Heidelberg, 1982).
[3] N. Esser and W. Richter, *Light Scattering in Solids VIII*, edited by M. Cardona and G. Güntherodt, Topics Appl. Phys. Vol. 76 (Springer-Verlag, Berlin, Heidelberg, 2000).
[4] B. Persson, On the theory of surface-enhanced Raman scattering, Chem. Phys. Lett. **82**, 561 (1981).
[5] S.-Y. Ding, E.-M. You, Z.-Q. Tian, and M. Moskovits, Electromagnetic theories of surface-enhanced Raman spectroscopy, Chem. Soc. Rev. **46**, 4042 (2017).
[6] M. Hünermann, J. Geurts, and W. Richter, Observation of Interface Phonons by Light Scattering from Epitaxial Sb Monolayers on III-V Semiconductors, Phys. Rev. Lett. **66**, 640 (1991).
[7] K. Hinrichs, A. Schierhorn, P. Haier, N. Esser, W. Richter, and J. Sahm, Surface Phonons of InP(110) Studied by Raman Spectroscopy, Phys. Rev. Lett. **79**, 1094 (1997).
[8] N. Esser and E. Speiser, *Physics of Solid Surfaces*, edited by G. Chiarotti and P. Chiaradia, Landolt-Börnstein: Numerical Data and Functional Relationships in Science and Technology—New Series Vol. 45B (Springer-Verlag, Berlin, Heidelberg, 2018).
[9] E. Speiser, N. Esser, B. Halbig, J. Geurts, W. G. Schmidt, and S. Sanna, Vibrational raman spectroscopy on adsorbate-induced low-dimensional surface structures, Surf. Sci. Rep. **75**, 100480 (2020).
[10] J. H. Parker, D. W. Feldman, and M. Ashkin, *Light Scattering Spectra of Solids*, edited by G. B. Wright (Springer-Verlag, New York, 1969).
[11] L. M. Fraas, S. P. S. Porto, and E. Loh, Symmetry in Raman scattering from the optical phonon in single crystal beryllium, Solid State Commun. **8**, 803 (1970).
[12] W. B. Grant, H. Schulz, S. Hüfner, and J. Pelzl, Investigation of $k = 0$ phonons in Bi, Cd, Mg, and Zn by Raman scattering, Phys. Status Solidi (b) **60**, 331 (1973).
[13] W.-D. Schöne and W. Ekardt, Time-dependent screening of a positive charge distribution in metals: Excitons on an ultrashort time scale, Phys. Rev. B **62**, 13464 (2000).
[14] W.-D. Schöne and W. Ekardt, Transient excitonic states in noble metals and Al, Phys. Rev. B **65**, 113112 (2002).
[15] F. Wang, D. J. Cho, B. Kessler, J. Deslippe, P. J. Schuck, S. G. Louie, A. Zettl, T. F. Heinz, and Y. R. Shen, Observation of Excitons in One-Dimensional Metallic Single-Walled Carbon Nanotubes, Phys. Rev. Lett. **99**, 227401 (2007).
[16] X. Cui, C. Wang, A. Argondizzo, S. Garrett-Roe, B. Gumhalter, and H. Petek, Transient excitons at metal surfaces, Nat. Phys. **10**, 505 (2014).
[17] S. Ogawa, H. Nagano, and H. Petek, Hot-electron dynamics at Cu(100), Cu(110), and Cu(111) surfaces: Comparison of experiment with Fermi-liquid theory, Phys. Rev. B **55**, 10869 (1997).
[18] M. Bayle, P. Benzo, N. Combe, C. Gatel, C. Bonafos, G. Benassayag, and R. Carles, Experimental investigation of the vibrational density of states and electronic excitations in metallic nanocrystals, Phys. Rev. B **89**, 195402 (2014).
[19] M. Bayle, N. Combe, N. M. Sangeetha, G. Viau, and R. Carles, Vibrational and electronic excitations in gold nanocrystals, Nanoscale **6**, 9157 (2014).
[20] S. Liu, B. Cirera, Y. Sun, I. Hamada, M. Müller, A. Hammud, M. Wolf, and T. Kumagai, Dramatic enhancement of tip-enhanced Raman scattering mediated by atomic point contact formation, Nano Lett. **20**, 5879 (2020).
[21] S. Liu, A. Hammud, M. Wolf, and T. Kumagai, Atomic point contact raman spectroscopy of a Si(111)- 7×7 surface, Nano Lett. **21**, 4057 (2021).
[22] See Supplemental Material at http://link.aps.org/supplemental/10.1103/PhysRevLett.128.216101, which includes Refs. [23–35], for details on experiments and calculations.
[23] L. D. Sun, M. Hohage, P. Zeppenfeld, R. E. Balderas-Navarro, and K. Hingerl, Enhanced Optical Sensitivity to Adsorption due to Depolarization of Anisotropic Surface States, Phys. Rev. Lett. **90**, 106104 (2003).
[24] L. D. Sun, M. Hohage, and P. Zeppenfeld, Optical probe for surface and subsurface defects induced by ion bombardment, Phys. Status Solidi RRL **7**, 301 (2013).
[25] P. B. Johnson and R. W. Christy, Optical constants of the noble metals, Phys. Rev. B **6**, 4370 (1972).
[26] D. E. Aspnes and A. A. Studna, Dielectric functions and optical parameters of Si, Ge, GaP, GaAs, GaSb, InP, InAs, and InSb from 1.5 to 6.0 eV, Phys. Rev. B **27**, 985 (1983).
[27] G. Kresse and J. Furthmüller, Efficiency of ab initio total energy calculations for metals and semiconductors using a plane-wave basis set, Comput. Mater. Sci. **6**, 15 (1996).

[28] G. Kresse and J. Furthmüller, Efficient iterative schemes for ab initio total-energy calculations using a plane-wave basis set, Phys. Rev. B **54**, 11169 (1996).
[29] G. Kresse and D. Joubert, From ultrasoft pseudopotentials to the projector augmented-wave method, Phys. Rev. B **59**, 1758 (1999).
[30] P. E. Blöchl, Projector augmented-wave method, Phys. Rev. B **50**, 17953 (1994).
[31] J. P. Perdew, A. Ruzsinszky, G. I. Csonka, O. A. Vydrov, G. E. Scuseria, L. A. Constantin, X. Zhou, and K. Burke, Restoring the Density-Gradient Expansion for Exchange in Solids and Surfaces, Phys. Rev. Lett. **100**, 136406 (2008).
[32] J. P. Perdew, J. A. Chevary, S. H. Vosko, K. A. Jackson, M. R. Pederson, D. J. Singh, and C. Fiolhais, Atoms, molecules, solids, and surfaces: Applications of the generalized gradient approximation for exchange and correlation, Phys. Rev. B **46**, 6671 (1992).
[33] R. P. Feynman, Forces in molecules, Phys. Rev. **56**, 340 (1939).
[34] H. J. Monkhorst and J. D. Pack, Special points for Brillouin-zone integrations, Phys. Rev. B **13**, 5188 (1976).
[35] K. H. Weyrich, "Frozen" phonon calculations: Lattice dynamics and -Instabilities, Ferroelectrics **104**, 183 (1990).
[36] J. A. Stroscio, M. Persson, S. R. Bare, and W. Ho, Observation of Structure-Induced Surface Vibrational Resonances on Metal Surfaces, Phys. Rev. Lett. **54**, 1428 (1985).
[37] P. Zeppenfeld, K. Kern, R. David, K. Kuhnke, and G. Comsa, Lattice dynamics of Cu(110): High-resolution He-scattering study, Phys. Rev. B **38**, 12329 (1988).
[38] M. Persson, J. A. Stroscio, and W. Ho, Geometric structure, pseudoband gaps, and surface vibrational resonances on metal surfaces, Phys. Scr. **36**, 548 (1987).
[39] S. Kevan, High-resolution angle-resolved photoemission study of the Cu(011) surface state, Phys. Rev. B **28**, 4822 (1983).
[40] A. Goldmann, V. Dose, and G. Borstel, Empty electronic states at the (100), (110), and (111) surfaces of nickel, copper, and silver, Phys. Rev. B **32**, 1971 (1985).
[41] A. Baghbanpourasl, W. G. Schmidt, M. Denk, C. Cobet, M. Hohage, P. Zeppenfeld, and K. Hingerl, Water adsorbate influence on the Cu(110) surface optical response, Surf. Sci. **641**, 231 (2015).
[42] P. Hofmann, K. C. Rose, V. Fernandez, A. M. Bradshaw, and W. Richter, Study of Surface States on Cu(110) Using Optical Reflectance Anisotropy, Phys. Rev. Lett. **75**, 2039 (1995).
[43] J.-K. Hansen, J. Bremer, and O. Hunderi, The electronic structure of Cu(110) and Ag(110) surfaces studied by reflection anisotropy spectroscopy, Surf. Sci. **418**, L58 (1998).
[44] L. D. Sun, M. Hohage, P. Zeppenfeld, and R. E. Balderas-Navarro, Origin and temperature dependence of the surface optical anisotropy on Cu(110), Surf. Sci. **589**, 153 (2005).
[45] J. Harl, G. Kresse, L. D. Sun, M. Hohage, and P. Zeppenfeld, Ab initio reflectance difference spectra of the bare and adsorbate covered Cu(110) surfaces, Phys. Rev. B **76**, 035436 (2007).
[46] R. L. Aggarwal, L. W. Farrar, S. K. Saikin, A. Aspuru-Guzik, M. Stopa, and D. L. Polla, Measurement of the absolute Raman cross section of the optical phonon in silicon, Solid State Commun. **151**, 553 (2011).